J Mol Model (2013) 19:131–138
DOI 10.1007/s00894-012-1533-x

ORIGINAL PAPER

Computational investigation on the new high energy density material of aluminum enriched 1, 1-diamino-2, 2-dinitroethylene

Liang Bian · Yuanjie Shu · Jinbao Xu · Lei Wang

Received: 16 May 2012 / Accepted: 8 July 2012 / Published online: 24 July 2012

Abstract Aluminum enriched 1, 1-diamino-2, 2-dinitroethylene (Al-FOX-7) crystal, as a new high energy density material (HEDM), was designed and investigated using grand canonical monte carlo (GCMC), NVT+NPT-molecular dynamics (MD) and GGA-PBE-density functional theory (DFT) methods. The results show that, Al atoms break out H-bond of functional group of FOX-7 crystal, and form new Al-H and Al-O bonds. Their atomic content (x) influences the surface electronic states, friction sensitivities and *cj* detonation properties of Al-FOX-7 crystals. While x is 4 atoms, the crystal has the highest friction sensitivities and *cj* detonation temperatures, which are about 1.5 times to that of FOX-7 crystal.

Keywords Aluminum 1 · Crystal · 1-diamino-2 · 2-dinitroethylene · First-principles · Molecular dynamics

Introduction

High density FOX-7 showed extreme detonation properties in CHON energetic materials [1, 2]. To obtain the higher detonation and sensitivity properties of FOX-7 crystal, the researchers studied the complex compounds, for example, Al enriched FOX-7 compounds [3]. In 2008, Makhov et al. [4] reported that the nanostructure aluminized composite can be superior to mechanical mixture in acceleration ability if the main explosive including FOX-7 had a highly negative oxygen balance. It indicates that the aluminized composite could enhance the detonation properties of FOX-7 crystal [5]. In Vadhe's review [6], the aluminum content must be optimized in the explosive powders. Higher aluminum content is incorporated in most of the compositions for a sustained blast effect, due to the potential of secondary reactions of Al atoms with detonation products. The authors argue that the small particle size of the aluminum tends to raise detonation velocity of explosive matrix.

At present, there has been a growing interest in investigating Al-FOX-7 compounds and their properties from a molecular point of view [7]. Sorescu et al. [8] performed the adsorption of FOX-7 molecules on the Al (111) or α-Al_2O_3 (0001) [9] surface using DFT. The authors noted that the binding energy of Al (or α-Al_2O_3)-FOX-7 depend on the energy barrier between FOX-7 and Al (or α-Al_2O_3). Al atoms are easy to bind with the functional group of FOX-7 molecules, such as $-NO_2$ and $-NH_2$. According to this result, adding-on Al atoms have a probability ratio to improve density and sensitivity of FOX-7 crystal. This prompted us to design and construct the new Al-FOX-7 crystal [10, 11]. Here, this work used grand canonical Monte Carlo (GCMC) and molecular dynamics (MD) to define the Al atomic distribution in FOX-7 crystal, and then carried out *ab initio* principle to optimize and describe the surface electronic states of Al-FOX-7 crystals [12–14]. The corresponding friction sensitivities and detonation properties were determined through calculating morphologies and *cj* detonation properties [15–18].

L. Bian (✉) · J. Xu · L. Wang
Xinjiang Key Laboratory of Electronic Information Materials and Devices, Xinjiang Technical Institute of Physics & Chemistry, Chinese Academy of Sciences,
Urumqi 830011, China
e-mail: bianliang555551@126.com

L. Bian
e-mail: bianliang@ms.xjb.ac.cn

Y. Shu
Institute of Chemicals Materials,
China Academy of Engineering Physics,
Mianyang 621900, China

Computational details

All simulations were performed using Materials studio and self-programming software on SGI workstations in China academy of engineering physics. In FOX-7 crystal, the adjacent FOX-7 molecules were constructed by the short range van der Waals energy or H-bond energy. The long range electrostatic energy influences the parallel arrangement of FOX-7 molecules [19], see Fig. 1. The corresponding free volumes (V_g) are made by the outer electronic layers of molecules. They provide the probability distribution sites for absorbing Al atoms [20], and were calculated via Eq. 1. Therein, the large free volumes exist in the middle area of three FOX-7 molecules, and the max Al atomic content (x) is 4 atoms.

$$P \approx \left(n_p k_B T\right)/\left(p_{ip} V_p\right) \approx \left[\left(n_g + n_p\right)k_B T\right]/\left(V_g + p_{ip} V_p\right) \quad (1)$$

Where P means pressure, T is temperature, p_{ip} means the probability of insertion for probes into FOX-7 crystal, n_p is the number of probes inserts into FOX-7 crystal, n_g means the number of gases, V_p means the volume of FOX-7 crystal, and V_g is the free volume.

Considering the high surface activity of Al atoms in FOX-7 crystal [8], this work used grand canonical Monte Carlo (GCMC) and 200 ps NVT+NPT-molecular dynamics (MD) to define on the Al atoms randomly embedded in FOX-7 crystal, as shown in Eq. 2 [21]. The relative probability distribution ratios and loading quantity (N) were calculated using Eq. 3 [22]. While the E_m term has the minimum energy, the system tends to be stable. And then, this work used density functional theory (DFT) in the gengeralized gradient approximation (GGA-PBE) to describe the system stability via calculating total energy (E), as seen in Eq. 4 [23–25]. Therein, E^{SF} term closes to zero point that ignores the interaction energy in stable crystal model. Potential energy (U^S term) and non-bond energy (E^{SS} term) depend on the binding energy and structural distortion. And the add-on Al atoms could reduce the E^{SS} term, which includes $E_{Al\text{-}O}+E_{Al\text{-}H}\text{-}E_{O\text{-}H}$. As is displayed in Fig. 2, the formation enthalpy of Al-FOX-7 is less than that of FOX-7, and reduces with Al atomic content (x) increasing. It belongs to the linear, and the slope is −52.21 eV·atoms^{-1}. This means that, owing to energy spontaneously transfering to the lowest energy point, x will tend to be 4 atoms in Al-FOX-7 crystal, and then stable [8].

$$\rho_m = C\exp(-\beta E_m) \quad (2)$$

$$F = \left[(\beta f V)^N/N!\right]\exp[-\beta N u_{\text{intra}}] \quad (3)$$

Where ρ_m means the density of m structure, the C shows the normalization constant, β is the reciprocal temperature, and E_m means the total energy of m structure. F shows the total fugacity, V means the volume of m structure, f is the relative fugacity, u_{intra} is the intramolecular chemical potential, and N is the loading quantity.

$$E = E^{SS} + U^S + E^{SF} \quad (4)$$

Where E shows total energy, U^S is potential energy, E^{SS} means non bond energy, and E^{SF} is the interaction energy.

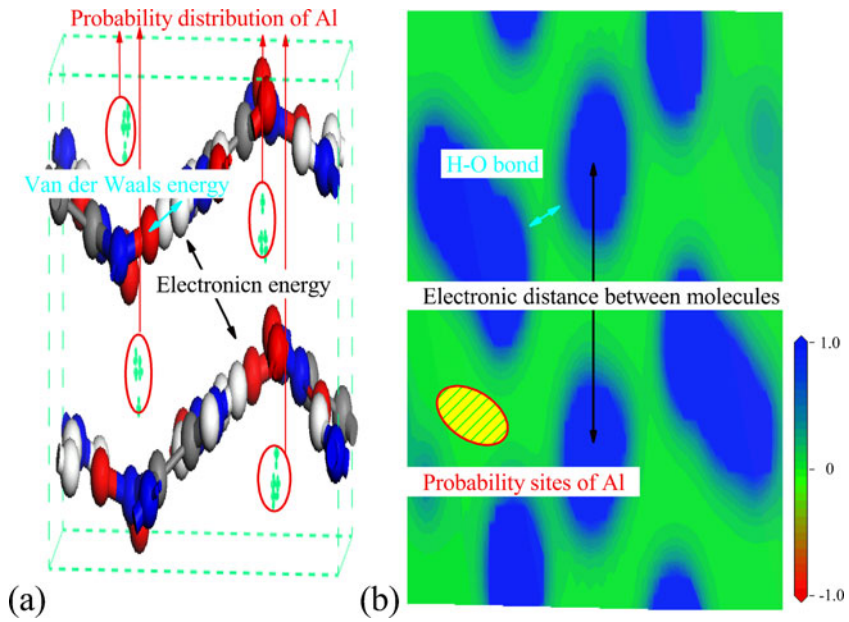

Fig. 1 Probability distributions ratios and sites of Al atoms in FOX-7 crystal. All the atoms followed the atomic non-bonded interaction function of COMPASS force filed. The Ewald+Group summation method for long range electrostatic interaction term was routinely used to evaluate the electrostatic interactions in reasonably small models

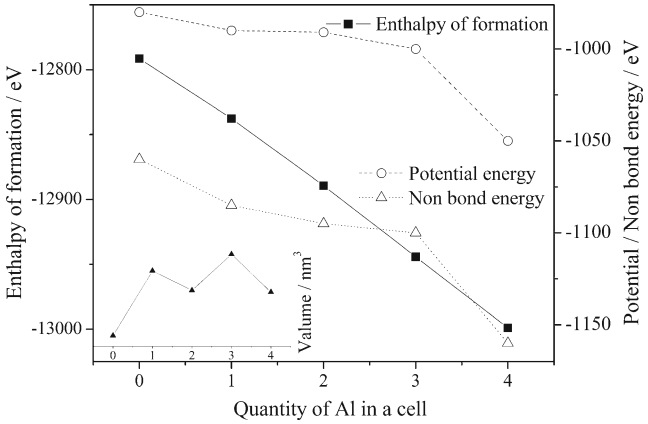

Fig. 2 Enthalpy of formation, potential energy and non bond energy of Al-FOX-7 crystals

In Al-FOX-7 crystal, Al atoms first enlarge the atomic distances of FOX-7 molecules along the parallel arrangement. The data of Table 1 shows that the Al atoms enlarge the lattice lengths of c axis. The relative crystal density decreases. However, 4Al-FOX-7 crystal (x=4) has the completely symmetric arrangement that leads long range electrostatic energy to increase. Thus, the density of system is a little higher than that of FOX-7 crystal. This will improve the *cj* detonation properties of FOX-7 crystal, such as cj pressure and cj velocity [5–7, 10]. Secondly, the add-on Al atoms approach to $-NH_2$, and break out the H-bonds between $-NO_2$ and $-NH_2$, as seen in Fig. 3. The new Al-O and Al-H bonds form that enlarges the atomic distances of the adjacent arrangement of FOX-7 molecules [8]. Finally, the H-bond lengths change with the Al-O and Al-H bonds increasing. According to Table 2, the Al-O and H-O bonds lengths tend to be homogeneous, respectively, and the overlapping electrons of system are considered as the U^S term in calculating the force field [8]. This needs to eliminate the E^{SS} term. The corresponding energy difference can be modified by the bond lengths decreasing, and reduces about 11 eV with one Al atom increasing [8, 9].

Once Al-FOX-7 crystal was determined, this work studied the friction sensitivities through calculating the growth ratios and crystal energies of crystal surfaces, using BFDH, growth morphology and equilibrium morphology methods [26]. They are related to the morphologies, which were simulated. Therein, the morphologies of Al-FOX-7 compounds are the same as that of FOX-7 crystal, because of the same space group (*P21/N*). In the BFDH method, the potential growth surfaces were isolated using the Donnay-Harker model [17]. Their growth ratios were deduced by Bravais-Friedel method [27]. Growth morphology method assumed that there was proportional for growth ratios and sorption energies. The (h k l) surface was calculated from the sorption energy using Donnay-Harker model. Finally, the morphology was obtained from Wuff pattern. Equilibrium morphology showed that the minimum surface energy was considered at 0 K. The surface energy was calculated from the given thickness finite lamina.

$$C_2H_4N_4O_4 \rightarrow H_2O + CO_2 + 2N_2 + H_2 + CO \quad (5)$$

$$2AlC_2H_4N_4O_4 \rightarrow H_2O + CO_2 + 4N_2 + 3H_2 + 2CO + C + Al_2O_3 \quad (6)$$

According to Mallard-Lechatelier (M-L) principle, FOX-7 and Al-FOX-7 crystals have complete decomposable products as explained in Eqs. 5 and 6. The relative detonation products are postulated as the following to calculate detonation properties. At first, all nitrogen atoms change to N_2. Secondly, oxygen atoms change to H_2O, while hydrogen atoms exist. Finally, carbon atoms change to CO or CO_2 if O atoms are surplus. Al atoms change to Al_2O_3 solid.

The detonation velocity (v_D) and detonation pressure (p_D) of Al-FOX-7 crystal were determined by Kamlet's formula using self-programming VLW software. They were expressed as ref [28]. It should be noted that these two detonation properties were calculated by heats of formation (HOF) of gas states, not of crystal. This HOF has a small effect on the heats of detonation (HOD) calculations. Specific impulse introduced by Politzer et al. [29]. Here, FOX-7 and Al-FOX-7 crystals were taken to calculate specific impulse. All detonation heats were used to heat the occurred gases. The pressure and enthalpy of combustion were constant when temperature changes from 298 K to T_c, and the velocities of gases appearing and disappearing were equal.

Table 1 Crystal parameters of Al-FOX-7 crystals. "*x*" means Al atomic content in Al-FOX-7 crystal

x	*a* (nm)	*b* (nm)	*c* (nm)	*β*(°)	Density (g·cm^{-3})
0	0.69	0.65	1.13	90.49	1.94
1	0.66	0.79	1.32	104.59	1.81
2	0.67	0.70	1.37	103.17	1.84
3	0.75	0.72	1.39	104.70	1.66
4	0.72	0.74	1.19	110.18	1.95

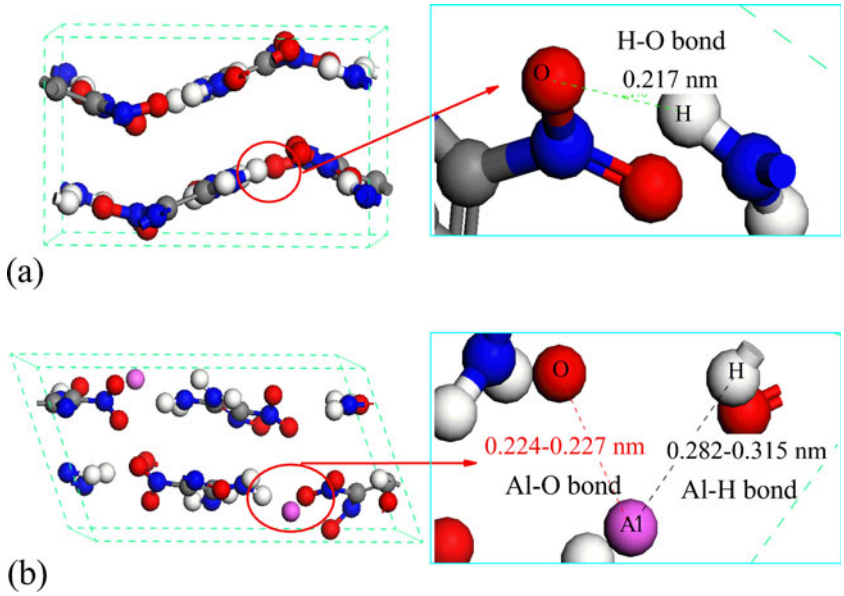

Fig. 3 Illustration of H-(Al)-O bond lengths of FOX-7 (**a**) and Al-FOX-7 (**b**) crystals. The space groups belong to P21/N

Results and discussion

Surface electronic states of Al-FOX-7 crystals

In Al-FOX-7 crystal, add-on Al atoms change the total atomic arrangements that lead the surface electronic states to warp. Figure 4a indicates that add-on Al atoms improve the total densities of states (DOS) moving away from Fermi energy, until stable states [4, 11]. This can be explained because the electronic energy of Al atoms reduces the total energy of the system, and the corresponding surface electronic densities depend on the Al atomic content (x), see Fig. 4b. When x is singular in Al-FOX-7 crystal, the surface electronic area of Al atoms is composed by 2p states. When add-on Al atoms are symmetrical in Al-FOX-7 crystal, the Al 2p states transmit to the electronic states of adjacent atoms. The total potential energy reduces [6]. This is close to the results of the enthalpy of formation.

Table 2 Binding energy differences and bond lengths of Al-FOX-7 crystals. "x" means the Al atomic content in Al-FOX-7 crystal

x	H-O (nm)	Al-H (nm)	Al-O (nm)	Binding energy differences (eV)
0	0.22	0	0	0
1	0.23–0.33	0.24–0.25	0.29–0.32	−3.69
2	0.22–0.32	0.27–0.32	0.29–0.32	−12.33
3	0.21–0.24	0.22–0.29	0.28–0.31	−23.25
4	0.19–0.22	0.25–0.32	0.30–0.32	−36.44

In order to obtain the influence of Al atoms in FOX-7 crystal, this work calculated the projection densities of states (PDOS) of Al-O and Al-H bonds, as shown in Fig. 5. These bonds belong to covalent bonds. Comparing to Al-O bonds, Al-H bonds change widely the ranges of PDOS intensities. It indicates that the atomic distances of Al-H bonds will tend to shorten and has been illustrated in Table 1. In the case of $x \leq 2$, the energy levels of Al-O and Al-H bonds depend on the electronic spin directions of Al 2p states which are the same as that of O 2p states. While x is more than 2, the electronic spin direction of Al 2p is opposite to that of O 2p states. The total density of p states reduces. This electronic transmission process depends on the heterozygous of Al-O bonds. Typically, 4Al-FOX-7 crystal (x=4) has the highest symmetry and the energy levels densities of Al-O and Al-H bonds are uniform and stable.

Friction sensitivities of Al-FOX-7 crystals

To obtain the friction sensitivity, this work investigated the crystal growth ratios through calculating morphology. The growth ratios (E_{latt}) were defined by the growth layer energies of d_{hkl} (E_{slice}) as in Eq. 7 [17, 18]. Therein, the low growth ratio is related to the high surface energy of crystal. While the low growth crystal surface is in compression by the frictional force, the decomposed ratio of surface molecules decreases. So the low growth crystal faces have high friction sensitivities.

$$E_{att} = E_{latt} - E_{slice} \tag{7}$$

Where E_{att} is crystal energy, E_{latt} shows growth rate, and E_{slice} means growth layer energy of d_{hkl}.

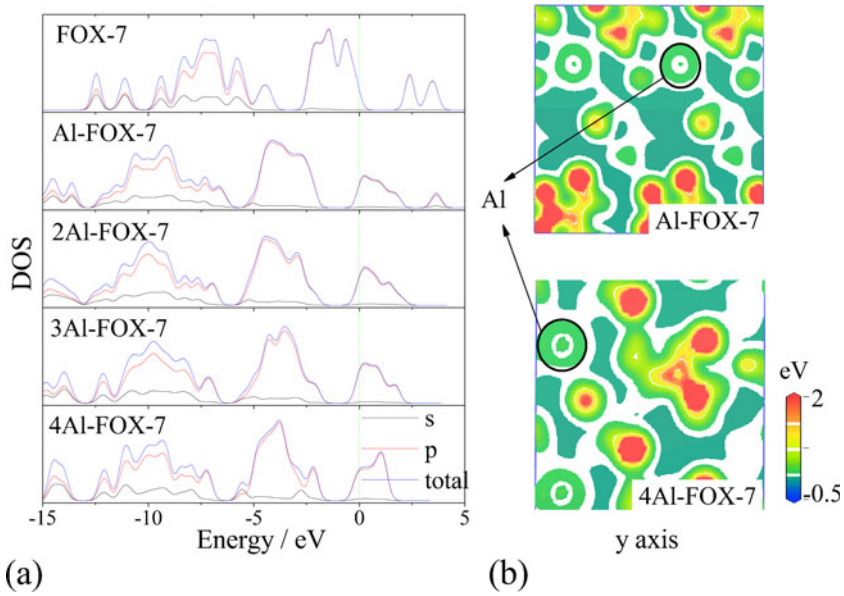

Fig. 4 Density of states (DOS) of Al-FOX-7 crystals (**a**) and their electronic density (**b**). Therein, (**b**) shows the cut plane along y axis

At present, there are three simulation methods for calculating morphology. Therein, BFDH models are just calculated according to (*h k l*) data. The data in Table 3 shows that, in BDFH morphology, the (*101*) face area of FOX-7 crystal is the maximum. However, the surface energy is ignored in the BFDH models. With the surface energy simulating, the growth faces have been solved using the growth morphology and equilibrium morphology models. While the sorption energy (E_{att}) is added into growth morphology in Table 4, the probable growth faces separated from the initial growth faces. It impels the friction sensitivities of (*111*) surfaces to increase.

Typically, the equilibrium morphology considers both surface area of crystal and its minimum energy. This method can simulate all the growth faces. Table 5 shows that Al atoms reduce the multiplics of FOX-7 crystal, until reaching geometric balances, and the $E_{surf\ (total)}$, $E_{surf\ (vdw)}$ and $E_{surf\ (elec)}$ terms change. Therein, the E_{att} term reduces and (*111*) surface energy (E_{surf}) enhances with Al atoms adding-on. This has been determined as the results in Fig. 2. Then, the E_{slice} term increases on the (*h k l*) surface, with add-on Al atoms increasing as in Table 5. It indicates that the Al atoms improve the friction sensitivity of FOX-7 crystal. This has been checked by reported data [18]. Specially, 4Al-FOX-7

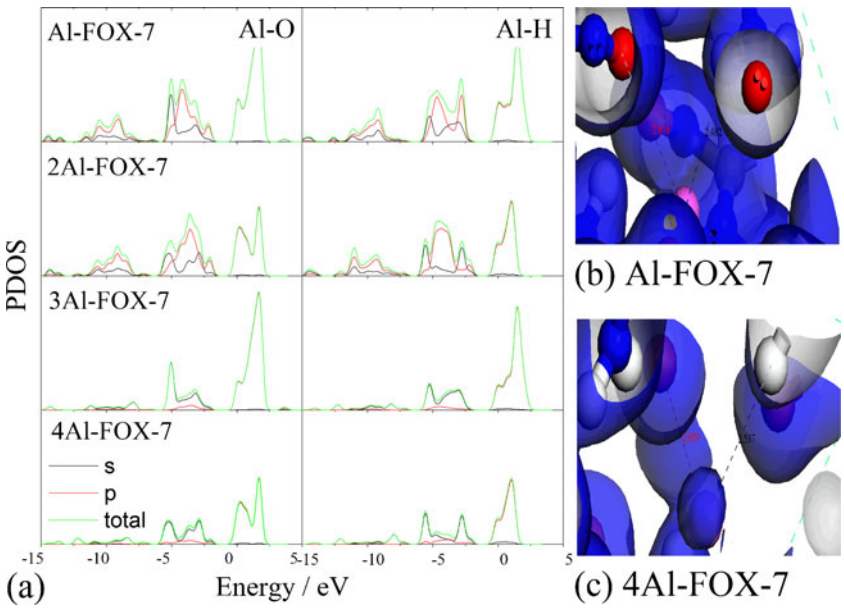

Fig. 5 Projected densities of states (PDOS) of Al-O and Al-H bonds of Al-FOX-7 crystal (**a**). The corresponding electronic densities of H-Al-O bonds are indicated as shown in Al-FOX-7 (**b**) and 4Al-FOX-7 (**c**) crystals

Table 3 BFDH morphology parameters of FOX-7 crystals

h k l	Multiplic	$d_{h\,k\,l}$	Total facet area	% Total facet area
001	2	17.76	737.61	13.84
101	2	17.02	1060	19.80
111	4	22.85	0.11	0.002

crystal has the lowest surface energy. Its E_{suef} and E_{elec} are about 1.5 times that of FOX-7 crystal. The corresponding friction sensitivity is the lowest. This phenomenon will be good for improving the friction sensitivity of FOX-7 crystal [17].

Besides, the primary crystal growth direction is along *y* axis. It is the first sensitive crystal face. The second growth face is along *xz* plat, which is the secondary sensitive crystal faces. Its growth directions further turn to *x* and *z* axis with Al atoms increasing. Consequently, the H-bonds of adjacent FOX-7 molecules first decompose along *y* axis [19, 23]. Secondly, the van der Waals forces of parallel FOX-7 molecules are damaged along *xz* plats, see Fig. 6. According to the arrow diagram in Fig. 6, this work calculated crystal growth ratios of Al-FOX-7 compounds via equilibrium morphology method. Along *y* axis, Al-FOX-7 crystal has higher growth ratios than FOX-7 crystal. The corresponding growth surfaces turn to *xz* plat, with the van der Waals force decreasing.

Detonation properties of Al-FOX-7 crystals

In the state equation, the detonation properties of Al-FOX-7 crystal depend on the crystal density. A high density crystal has high detonation velocity and pressure. The calculated *cj* parameters of Al-FOX-7 crystals close to the reported data of Al (or Al_2O_3) enriched FOX-7 mixtures [5, 28]. As illustrated in Fig. 7, the *cj* volumes of Al-FOX-7 crystal are the same as that of crystal FOX-7. The relative detonation velocity and pressure are a direct ratio with the crystal densities. While FOX-7 molecules first decompose [6, 18], the gaseous products include the decomposed products of FOX-7 molecules, and solid products (Al_2O_3) have little effect on the gaseous products. With the Al_2O_3 solids increasing, the *cj* velocity and *cj* pressure of Al-FOX-7 will decrease. Although the density of crystal 4Al-FOX-7 (1.95 $g{\cdot}cm^{-3}$) is higher than that of FOX-7 crystal (1.94 $g{\cdot}cm^{-3}$), the data of *cj* velocity and *cj* pressure are a little less [5, 6]. They are 42.16 GPa and 9230 $m{\cdot}s^{-1}$, respectively.

Moreover, add-on Al atoms improve the uniformly hot-energy transfers between adjacent atoms via heterozygous electrons on p states [11, 13]. They obviously increase the detonation temperature of Al-FOX-7. The *cj* temperature data of Al-FOX-7 are fitted as linear, and the slope is 608.84 ° K·Al $atoms^{-1}$, see Fig. 7. Typically, 4Al-FOX-7 crystal provides enough Al atoms to transfer the uniform hot-energy while FOX-7 molecules absorb the excitation energy until decomposing. It has the highest *cj* detonation temperature which is 1.5 times that of FOX-7 crystal [2, 3].

It is worthy to note that, in the present paper, the data of *cj* velocity and *cj* pressure are the static data, which ignores the second-order thermite reaction. In the real dynamic detonation process, Al atoms will add the hot spot into the decomposed process. Hot spot theory shows, described by Vandersall et al. [30], the "hot spot" consumes the surrounding explosive particles at reduced reaction rates, and causes longer distances to detonation. This enlarges the detonation range, and is usually considered in the detonation properties in the

Table 4 Surface energies of FOX-7 crystals in growth morphology models. Units: eV

h k l	Multiplic	$d_{h\,k\,l}$	*Eatt* (total)	*Eatt* (vdw)	*Eatt* (elec)	Total facet area	% Total facet area
001	2	30.80	−38.12	−26.20	−11.92	639.46	4.58
101	2	38.12	−30.80	−20.53	−10.27	2480	17.74
111	4	29.62	−29.62	−29.08	−0.54	1570	11.25

Table 5 Surface energies of Al-FOX-7 crystals in equilibrium morphology models. Units: eV

x	*h k l*	Multiplic	$d_{h\,k\,l}$	*Esurf* (total)	*Esurf* (vdw)	*Esurf* (elec)	Total facet area	% Total facet area
0	001	2	221.77	0.22	0.13	0.09	682.51	0.18
	101	2	188.23	0.19	0.12	0.06	15000	3.93
	111	4	140.19	0.14	0.14	0.002	84100	22.05
1	001	1	182.16	0.18	0.13	0.05	63200	10.47
	101	1	217.45	0.22	0.14	0.07	9790	1.62
	111	1	160.11	0.16	0.12	0.04	49600	8.22
2	001	1	246.99	0.25	0.14	0.10	23500	3.36
	101	1	218.69	0.22	0.15	0.07	20000	2.85
	111	1	231.03	0.23	0.13	0.09	16200	2.32
3	001	1	191.53	0.19	0.08	0.11	46600	8.45
	101	1	215.98	0.22	0.17	0.05	2540	0.46
	111	1	221.30	0.22	0.14	0.08	2380	0.43
4	001	2	304.97	0.30	0.19	0.11	134000	10.64
	101	2	351.25	0.35	0.19	0.16	10000	0.79
	111	4	293.61	0.29	0.21	0.08	61600	4.87

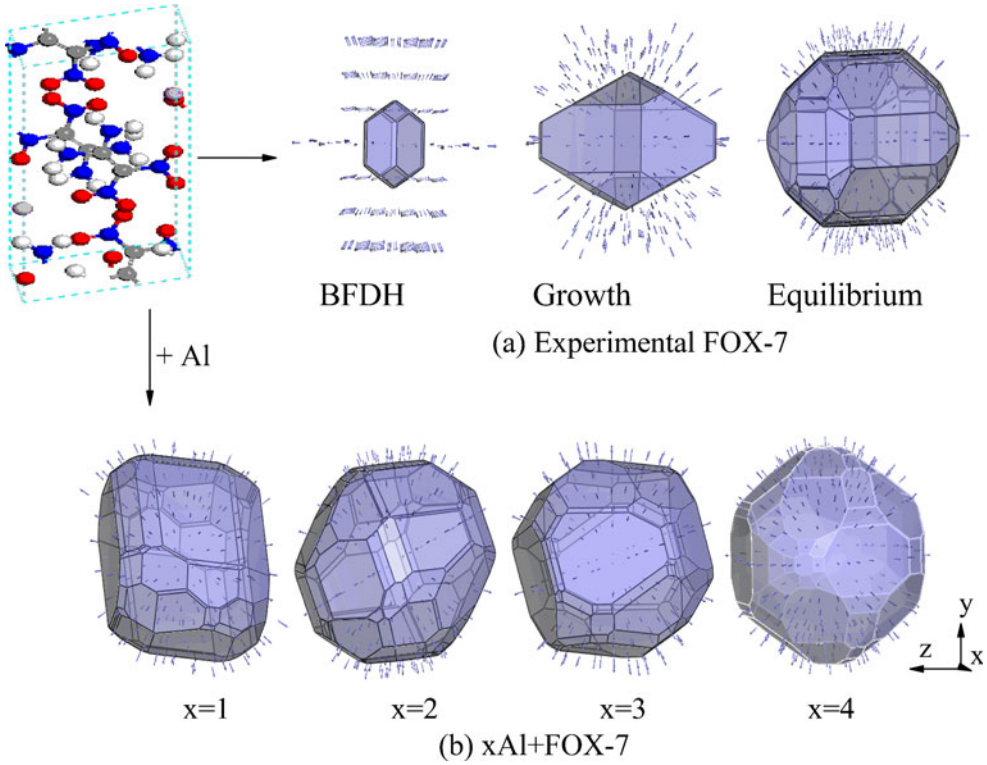

Fig. 6 Morphologies of FOX-7 and Al-FOX-7 crystals. Therein, the arrow shows the growth direction. Its density means the growth ratios. The "*x*" means the Al atomic content in Al-FOX-7 crystal

experimental detection [5]. Consequently, the dynamic detonation properties of Al-FOX-7 crystals will be better than the calculated static data [5, 10].

Conclusions

A new HEDM, namely Al-FOX-7 crystal, was designed and developed for improving the friction sensitivity and detonation property of FOX-7 crystal. At first, GCMC, MD and DFT calculations were used to describe the structural properties of Al-FOX-7 crystal. The results show that, add-on Al atoms form new Al-H and Al-O bonds with $-NO_2$ and $-NH_2$ of FOX-7 crystal that increase the lattice lengths. These are close to the results of DOS and PDOS. Secondly, to obtain the friction sensitivity of Al-FOX-7 crystal, this work used equilibrium morphology model to describe the surface growth property. The chief decomposed direction is along y axis. With Al atoms adding-on, the decomposed directions of Al-FOX-7 crystal turn to *xz* plat. Finally, this work used the state equation to calculate and discuss the relative detonation property and Al atomic content (*x*) influencing. Add-on Al atoms obviously improve the *cj* detonation temperature of crystal FOX-7; however, they reduce the *cj* velocity and *cj* pressure. In short, 4Al-FOX-7 crystal has the highest friction sensitivities and detonation temperatures, which are about 1.5 times that of FOX-7 crystal. The corresponding data of *cj* pressure and *cj* velocity are close to that of FOX-7 crystal.

This work demonstrates how Al atoms influence the friction sensitivities and detonation properties of FOX-7 crystal, but this work just calculated the static data of Al-FOX-7 crystal. Further theoretical studies should also include the dynamic process of Al-FOX-7 crystal, in order to better predict and correct the total properties of system. This work, however, provides useful information on how to design a new HEDM, and on understanding the relations of structure, sensitivity and *cj* detonation properties.

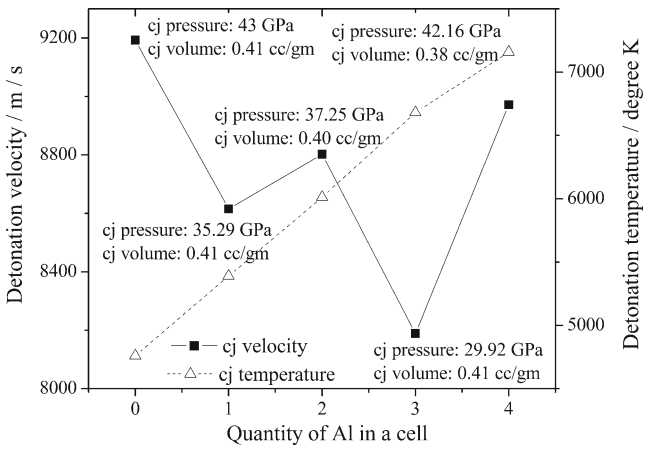

Fig. 7 Cj detonation properties of FOX-7 and Al-FOX-7 crystals, including *cj* pressure, *cj* volume, *cj* velocity and *cj* temperature

Acknowledgments This work was supported by the national natural science foundation (11011120241 and 11076002), the One Hundred Talents Project Foundation Program, the Western Light Joint Scholar Foundation Program of Chinese Academy of Sciences (Y12S311301), Youth Science Foundation of Xinjiang Uygur Autonomous Region of China (2011211B49), State 863 projects (2009AA050703) and the National Defense Basic Research Foundation of China (2006A099).

References

1. Gindulyte A, Massa L (1999) Proposed mechanism of 1,1-diamino-dinitroethylene decomposition: a density functional theory study. J Phys Chem 101:4375–4383
2. Zerilli FJ, Kuklja MM (2007) *Ab initio* equation of state of an organic molecular crystal: 1,1-Diamino-2,2-dinitroethylene. J Phys Chem A 111:1721–1725
3. Xu KZ, Song JR, Zhao FQ et al. (2008) Thermal behavior, specific heat capacity and adiabatic time-to-explosion of G(FOX-7). J Hazard Mater 158:333–339
4. Makhov MN, Arkhipov VI (2008) Method for estimating the acceleration ability of aluminized high explosives. Russian J Phys Chem B 2:602–608
5. Kresse G, Hafner J (1994) Norm-conserving and ultrasoft pseudopotentials for first-row and transition elements. Phys Rev B 49:14251–14269
6. Vadhe PP, Pawar RB, Sinha RK et al. (2008) Cast aluminized explosives (review). Combust Explo Shock 44:461–477
7. Raugei S, Klein ML (2001) Dynamics of water molecules in the Br- solvation shell: an *ab initio* molecular dynamics study. J Am Chem Soc 123:9484–9485
8. Sorescu DC, Boatz JA, Thompson DL (2003) First-principles calculations of the adsorption of nitromethane and 1,1-Diamino-2,2-dinitroethylene (FOX-7) molecules on the Al(111) surface. J Phys Chem B 107:8953–8964
9. Sorescu DC, Boatz JA, Thompson DL (2005) First-principles calculations of the adsorption of nitromethane and 1, 1-Diamino-2, 2-dinitroethylene (FOX-7) molecules on the α-Al_2O_3 (0001) surface. J Phys Chem B 109:1451–1463
10. Trzciński WA, Cudziło S, Szymańczyk L (2007) Studies of detonation characteristics of aluminum enriched RDX compositions. Propell Explos Pyrot 32:392–400
11. Ballone P, Andreoni W, Car R et al. (1988) Equilibrium structures and finite temperature properties of silicon microclusters from *ab initio* molecular-dynamics calculations. Phys Rev Lett 60:271–274
12. Williams RW, Malhotra D (2006) Van der Waals corrections to density functional theory calculations: Methane, ethane, ethylene, benzene, formaldehyde, ammonia, water, PBE, and CPMD. Chem Phys 327:54–62
13. Qiu L, Xiao HM, Zhu WH et al. (2006) *Ab initio* and molecular dynamics studies of crystalline TNAD (trans-1, 4, 5, 8-Tetranitro-1, 4, 5, 8-tetraazadecalin). J Phys Chem B 110:10651–10661
14. Isayev O, Gorb L, Qasim M et al. (2008) *Ab initio* molecular dynamics study on the initial chemical events in nitramines: thermal decomposition of CL-20. J Phys Chem B 112:11005–11013
15. Gogulya MF, Brazhnikov MA (2010) Pressure and temperature of the detonation products of explosive materials containing aluminum of various dispersities. Russian J Phys Chem B 29:773–787
16. Das A, Ji S, Fan Z (2002) Morphological development of solidification structures under forced fluid flow: a Monte-Carlo simulation. Acta Mater 50:4571–4585
17. Bénazet S, Jacob G, Pèpe G (2009) GenMol^{TM} supramolecular descriptors predicting reliable sensitivity of energetic compounds. Propell Explos Pyrot 34:120–135
18. Kuklja MM, Rashkeev SN, Zerilli FJ (2006) Shear-strain induced decomposition of 1, 1-diamino-2, 2-dinitroethylene. Appl Phys Lett 89:071904–071906
19. Rashkeev SN, Kuklja MM, Zerilli FJ (2003) Electronic excitations and decomposition of 1, 1-diamino-2, 2-dinitroethylene. Appl Phys Lett 82:1371–1378
20. Fuchs K, Friedrich C, Weese J (1996) Viscoelastic Properties of Narrow-Distribution Poly (methyl methacrylates). Macromolecules 29:5893–5901
21. Sorescu DC, Boatz JA, Thompson DL (2001) Classical and quantum-mechanical studies of crystalline FOX-7 (1,1-Diamino-2,2-dinitroethylene). J Phys Chem A 105:5010–5021
22. Merchant ME (2009) Mechanics of the metal cutting process II plasticity conditions in orthogonal cutting. J Appl Phys 16:267–275
23. Kuklja MM, Rashkeev SN (2007) Shear-strain-induced structural and electronic modifications of the molecular crystal 1, 1-diamino-2, 2-dinitroethylene: Slip-plane flow and band gap relaxation. Phys Rev B 75:104111–104120
24. Zhang CY, Wang XC, Huang H (2008) π-Stacked interactions in explosive crystals: buffers against external mechanical stimuli. J Am Chem Soc 130:8359–8365
25. Prywer J (2004) Explanation of some peculiarities of crystal morphology deduced from the BFDH law. J Cryst Growth 270:699–710
26. Kaminsky W, Responte D, Daranciang D et al. (2010) Structure, morphology and optical properties of chiral N-(4-X-phenyl)-N-[1 (S)-1-phenylethyl] thiourea, X=Cl, Br, and NO_2. Molecular 15:554–569
27. Zhang CY, Shu YJ, Zhao XD et al. (2005) Computational investigation on HEDM of azoic and azoxy derivatives of DAF, FOX-7, TATB, ANPZ and LLM-105. THEOCHEM 728:129–134
28. Zhou SQ, Zhao FQ, Ju XH et al. (2010) A density functional theory study of adsorption and decomposition of nitroamine molecules on the Al (111) surface. J Phys Chem C 114:9390–9397
29. Politzer P, Lane P, Murray JS (2011) Computational characterization of a potential energetic compound: 1,3,5,7-tetranitro-2,4,6,8-tetraazacubane. Cent European J Energ Mater 8:39–52
30. Vandersall KS, Tarver CM, Garcia F et al. (2010) On the low pressure shock initiation of octahydro-1,3,5,7–tetranitro-1,3,5,7-tetrazocine based plastic bonded explosives. J Appl Phys 107:094906–094911